CrystEngComm

Accepted Manuscript

ROYAL SOCIETY OF CHEMISTRY

www.rsc.org/crystengcomm

Solvent effects in solvo-hydrothermal synthesis of uranyl ion complexes with 1,3-adamantanediacetate†

Pierre Thuéry[a] and Jack Harrowfield[b]

[a] *CEA, IRAMIS, CNRS UMR 3685 NIMBE, LCMCE, Bât. 125, 91191 Gif-sur-Yvette, France. E-mail: pierre.thuery@cea.fr*

[b] *ISIS, Université de Strasbourg, 8 allée Gaspard Monge, 67083 Strasbourg, France. E-mail: harrowfield@unistra.fr*

1,3-Adamantanediacetic acid (H_2ADA) was reacted with uranyl nitrate under solvo-hydrothermal conditions with different organic solvents, giving five complexes which were characterized by their crystal structures and, in most cases, their luminescence properties. The complexes $[UO_2(ADA)(H_2O)]$ (**1**) and $[UO_2(ADA)(NMP)]$ (**2**), where NMP is *N*-methyl-2-pyrrolidone, are ribbon-like 1D coordination polymers including doubly carboxylate-bridged uranyl dimers, with the carboxylate groups being either chelating or bridging bidentate. The denticity of the ADA^{2-} ligand is greater in complex **3**, $[UO_2(ADA)]\cdot0.5CH_3CN$, which crystallizes as a planar 2D network with no coordinated solvent. Two complexes were obtained in water/*N,N*-dimethylformamide (DMF), which both display 2D arrangements. The topology in $[UO_2(ADA)(DMF)]$ (**4**) appears to stem from that of the ribbons in **1** and **2** through diversion of the bonds of every other dimer toward adjacent ribbons. The complex $[H_2NMe_2]_2[(UO_2)_2(ADA)_3]\cdot3H_2O$ (**5**) includes dimethylammonium counter-ions formed in situ from DMF hydrolysis. All ligands in **5** are bis-chelating and the anionic 2D assembly formed, which comprises 8- and 16-membered rings, is ~15 Å thick, half the uranyl ions having their equatorial plane approximately parallel and the other half perpendicular to the sheet plane; adjacent sheets are linked by hydrogen bonded cyclic water hexamers. Emission spectra measured in the solid state show the usual vibronic fine structure, the positions of the maxima reflecting the differences in the number of equatorial donors.

† CCDC reference numbers 1047136–1047140. For crystallographic data in CIF or other electronic format see DOI:

Introduction

In the course of an investigation of uranyl–organic coordination polymers or frameworks[1] with cyclohexyl-based polycarboxylate ligands, we have reported in recent years the synthesis and crystal structures of compounds involving various derivatives bearing from two to six carboxylate groups and displaying different geometries and flexibilities.[2–9] As usual with uranyl compounds, 1D and 2D architectures abound in this family, for example in the complexes obtained with cyclohexane-1,3-dicarboxylic,[2] all-*cis* 1,2,3,4,5,6-cyclohexanehexacarboxylic (with additional lanthanide cations)[3] or bicyclo[2.2.2]oct-7-ene-2,3,5,6-tetracarboxylic acids.[4] With di- or tricarboxylic acids possessing convergent binding groups (a property which differentiates these alicyclic ligands from their more often used aromatic counterparts[10]), more original polynuclear complexes, box- or capsule-shaped, can be generated, for example with Kemp's triacid (*cis*,*cis*-1,3,5-trimethylcyclohexane-1,3,5-tricarboxylic acid) or its derivatives.[5–7] Nanotubular species also were found in the cases of Kemp's triacid[6] and 1,3,5-cyclohexanetricarboxylic acid,[8] as well as a 3D framework in the latter case. More recently, 1,3-adamantanedicarboxylic acid was shown to give 1D to 3D polymers with uranyl ions alone or in combination with 3d block metal ions.[9] This indication of the influence of the scaffolding separating the two carboxylate donors seemed to us worthy of further investigation by increasing its size and flexibility and thus we have now used 1,3-adamantanediacetic acid as a ligand source to obtain five complexes which have been characterized by their crystal structures and, in most cases, their emission spectra at ambient temperature. These complexes were synthesized under solvo-hydrothermal conditions using different organic solvent components, which has previously been found to be a way to generate different species from a single uranyl/ligand system, and also to prevent oligomerisation through hydrolysis.[6–9,11]

Experimental

Synthesis

Caution! Uranium is a radioactive and chemically toxic element, and uranium-containing samples must be handled with suitable care and protection.

$UO_2(NO_3)_2\cdot 6H_2O$ (depleted uranium, R. P. Normapur, 99%) was purchased from Prolabo, and 1,3-adamantanediacetic acid (H_2ADA) from Aldrich. Elemental analyses were performed by MEDAC Ltd. at Chobham, UK.

$[UO_2(ADA)(H_2O)]$ (**1**). H_2ADA (13 mg, 0.05 mmol), $UO_2(NO_3)_2\cdot 6H_2O$ (25 mg, 0.05 mmol), acetonitrile (0.2 mL), and demineralized water (0.6 mL) were placed in a 15 mL tightly closed glass vessel and heated at 140 °C under autogenous pressure, giving light yellow crystals of complex **1** within three days (14 mg, 52% yield). Anal. calcd for $C_{14}H_{20}O_7U$: C, 31.24; H, 3.74. Found: C, 31.29; H, 3.44%.

$[UO_2(ADA)(NMP)]$ (**2**). H_2ADA (13 mg, 0.05 mmol), $UO_2(NO_3)_2\cdot 6H_2O$ (25 mg, 0.05 mmol), *N*-methyl-2-pyrrolidone (0.3 mL), and demineralized water (0.7 mL) were placed in a 15 mL tightly closed glass vessel and heated at 140 °C under autogenous pressure, giving light yellow crystals of complex **2** overnight (19 mg, 61% yield). Anal. calcd for $C_{19}H_{27}NO_7U$: C, 36.84; H, 4.39; N, 2.26. Found: C, 36.91; H, 4.28; N, 2.24%.

$[UO_2(ADA)]\cdot 0.5CH_3CN$ (**3**). H_2ADA (13 mg, 0.05 mmol), $UO_2(NO_3)_2\cdot 6H_2O$ (25 mg, 0.05 mmol), $Gd(NO_3)_3\cdot 6H_2O$ (23 mg, 0.05 mmol), acetonitrile (0.2 mL), and demineralized water

(0.7 mL) were placed in a 15 mL tightly closed glass vessel and heated at 140 °C under autogenous pressure. No solid appeared during the heating phase, but light yellow crystals of complex **3** were formed in low yield upon cooling the solution.

$[UO_2(ADA)(DMF)]$ (**4**). H_2ADA (13 mg, 0.05 mmol), $UO_2(NO_3)_2 \cdot 6H_2O$ (25 mg, 0.05 mmol), $Cu(NO_3)_2 \cdot 2.5H_2O$ (12 mg, 0.05 mmol), *N,N*-dimethylformamide (0.2 mL), and demineralized water (0.5 mL) were placed in a 15 mL tightly closed glass vessel and heated at 140 °C under autogenous pressure, giving light yellow crystals of complex **4** within three days (16 mg, 54% yield). Anal. calcd for $C_{17}H_{25}NO_7U$: C, 34.41; H, 4.25; N, 2.36. Found: C, 34.34; H, 4.04; N, 2.31%.

$[H_2NMe_2]_2[(UO_2)_2(ADA)_3] \cdot 3H_2O$ (**5**). H_2ADA (13 mg, 0.05 mmol), $UO_2(NO_3)_2 \cdot 6H_2O$ (25 mg, 0.05 mmol), *N,N*-dimethylformamide (0.2 mL), and demineralized water (0.5 mL) were placed in a 15 mL tightly closed glass vessel and heated at 140 °C under autogenous pressure, giving light yellow crystals of complex **5** within one week (15 mg, 63% yield based on the acid). Anal. calcd for $C_{46}H_{76}N_2O_{19}U_2$: C, 38.44; H, 5.33; N, 1.95. Found: C, 38.74; H, 5.02; N, 2.04%.

Crystallography

The data were collected at 150(2) K on a Nonius Kappa-CCD area detector diffractometer[12] using graphite-monochromated Mo Kα radiation (λ = 0.71073 Å). The crystals were introduced into glass capillaries with a protective coating of Paratone-N oil (Hampton Research). The unit cell parameters were determined from ten frames, then refined on all data. The data (combinations of φ- and ω-scans with a minimum redundancy of 4 for 90% of the reflections) were processed with HKL2000.[13] Absorption effects were corrected empirically with the program SCALEPACK.[13] The structures were solved either by usual direct methods with SHELXS[14] or by intrinsic phasing with SHELXT,[15] expanded when necessary by subsequent difference Fourier synthesis and refined by full-matrix least-squares on F^2 with SHELXL-2014.[16] All non-hydrogen atoms were refined with anisotropic displacement parameters. The hydrogen atoms bound to oxygen and nitrogen atoms were found on difference Fourier maps and the carbon-bound hydrogen atoms were introduced at calculated positions. All hydrogen atoms were treated as riding atoms with an isotropic displacement parameter equal to 1.2 times that of the parent atom (1.5 for CH_3, with optimized geometry). In complex **2**, the NMP molecule is disordered over two positions sharing atom O7, which were refined with occupancy parameters constrained to sum to unity. In complex **3**, a large residual electron density peak (ca 8 e $Å^{-3}$) is located very close to the uranium atom U1; this peak was observed for two crystals with very different shapes, which suggests that it is not an effect of imperfect absorption corrections, and it has been assumed that it represents a very minor component of the uranium atom, U2, with an occupancy factor which was first refined to 0.09, and then fixed to this value (since it was quite unstable during refinement); the low value of this occupancy explains why the corresponding positions for the coordinated oxygen atoms are not resolved. The acetonitrile solvent molecule in **3** is close to its image by symmetry and has thus been given an occupancy factor of 0.5.

Crystal data and structure refinement parameters are given in Table 1. The molecular plots were drawn with ORTEP-3[17] and the polyhedral representations with VESTA.[18] The topological analyses were made with TOPOS.[19]

Luminescence measurements. Emission spectra were recorded on solid samples using a Horiba-Jobin-Yvon Fluorolog spectrofluorimeter. Powdered complex was pressed between two silica plates which were mounted such that the faces were oriented vertically and at 45° to the incident excitation radiation. An excitation wavelength of 420 nm was used in all cases and the emissions monitored between 450 and 650 nm.

Results and discussion

Synthesis

Complexes **1**–**5** were synthesized under solvo-hydrothermal conditions at 140 °C (a value in the middle of the range of temperatures commonly employed). All crystals appeared during the heating phase, except for those of complex **3** which were formed on cooling the solution, and their presence in the glass vials was checked visually. The organic solvents for which crystalline materials could be obtained were acetonitrile for complexes **1** and **3**, *N*-methyl-2-pyrrolidone (NMP) for **2**, and *N,N*-dimethylformamide (DMF) for **4** and **5**. Acetonitrile is either absent from the final product (**1**) or present as a solvent in the lattice (**3**), whereas NMP and DMF are coordinated in **2** and **4**, respectively. In contrast to NMP, which is stable at the temperature used, DMF is readily hydrolysed into formic acid and dimethylamine, as previously documented,[20] and dimethylammonium cations are present in **5** as a result. Although the formation of oxo or hydroxo bridges is very frequent in uranyl aqueous chemistry,[1,21] this is not observed here, in keeping with previous observations of hydrolysis being in some measure prevented when solvo-hydrothermal conditions are used instead of purely hydrothermal ones.[6,7,9,11,22] Additional metal cations were introduced in the syntheses of **3** (Gd^{3+}) and **4** (Cu^{2+}), in the hope of obtaining heterometallic complexes of possibly higher dimensionality, but these cations are absent from the final products, although it is notable that, in both cases, the latter are different from the species formed in the absence of these cations (complexes **1** and **5**, respectively).

Crystal Structures

The structures of complexes $[UO_2(ADA)(H_2O)]$ (**1**) and $[UO_2(ADA)(NMP)]$ (**2**) are very similar to one another. In both cases, one of the carboxylate groups is chelating and the other is bridging bidentate, a coordination mode which has also been found in several uranyl ion complexes of 1,3-adamantanedicarboxylate (ADC^{2-}).[9,23] The uranyl cation is bound to four oxygen atoms from three carboxylate groups pertaining to three different ligands and to one terminal ligand, water in **1** (Fig. 1) or NMP in **2** (Fig. 2). As in all the complexes in the present series, the uranium atom is in a pentagonal bipyramidal environment. The U–O(carboxylate) bond lengths in **1** and **2** are in the ranges 2.452(2)–2.465(2) Å [average 2.459(5) Å] for chelating groups and 2.276(3)–2.363(2) Å [average 2.32(3) Å] for bridging bidentate ones, these values being unexceptional, as are those with the terminal ligands [2.434(3) and 2.364(2) Å for water and NMP, respectively]. In both compounds, doubly carboxylate-bridged, centrosymmetric uranyl dimers are formed, which are connected to one another through the chelating groups of the ligands and thus assembled into 1D coordination polymers running along the *b* and *a* axes in **1** and **2**, respectively. A similar arrangement, with the total point (Schläfli) symbol $\{4^2.6\}$ was found in the $[UO_2(ADC)L]$ complexes (L = H_2O or DMF).[9,23] However, whereas the terminal ligands project from both edges of the ribbons in **2** and the ADC^{2-} complexes, the water molecules in **1** are in the middle of the ribbons and protrude above and below. These water molecules form hydrogen bonds with the oxo atom O2 of a neighbouring uranyl group in the same chain, giving an $R_2^2(8)$ pattern in graph set notation,[24] and the carboxylate atom O4 from an adjoining chain along the *a* axis, giving a C(4) chain arrangement, both patterns including uranium centres [$O7\cdots O2^j$ 2.779(3) Å, $O7–H\cdots O2^j$ 154°, j = $-x$, $1 - y$, $1 - z$; $O7\cdots O4^l$ 2.709(4) Å, $O7–H\cdots O4^l$ 133°, l = $x - 1$, y, z]. The packings reflect these differences: the ribbons with lateral ADA^{2-} anions form hydrogen-bonded layers parallel to (0 0 1) and adjoining one another through their hydrophobic parts in **1**, while the more compact ribbons in **2** are stacked in a staggered-rows fashion. The Kitaigorodski packing indices (KPIs, estimated with PLATON[25]) for **1** and **2** are essentially identical (0.69 and 0.68, respectively) and they indicate that no significant free space is present.

The three complexes **3–5** crystallize as 2D networks, but their topologies are different. In [UO$_2$(ADA)(DMF)] (**4**), the bonding mode of the ADA^{2-} anion, with one chelating and one bridging bidentate carboxylate groups, is the same as in **1** and **2**, while in [UO$_2$(ADA)]·0.5CH$_3$CN (**3**), one oxygen atom of the chelating group is additionally bound to a second metal centre (Fig. 3). The fifth equatorial position in **4** is occupied instead by a DMF donor (Fig. 4). The U–O(carboxylate) bond lengths for the chelating group in **3** are 2.474(2) and 2.531(2) Å, the latter for the bridging atom O4 which makes another bond at 2.414(2) Å. The other bond lengths are unexceptional [2.442(10) and 2.455(10) Å for the chelating group in **4**, 2.259(2)–2.406(10) Å for the bridging bidentate groups in both compounds, and 2.371(11) Å with DMF]. The bidentate nature of atom O4 in **3** results in the formation of centrosymmetric uranium dimers with edge-sharing coordination polyhedra. These dimers are further assembled into a 2D network parallel to (0 0 1) and displaying rows of doubly bridged dimers running along the *b* axis, separated by rows of adamantyl skeletons, with the total point symbol $\{4^4.6^2\}$. These sheets are stacked in bump-to-hollow fashion, with a KPI index of 0.63 (disordered solvent excluded). In complex **4**, doubly carboxylate-bridged centrosymmetric dimers analogous to those in **1** and **2** are formed and they are assembled into a 2D assembly parallel to $(1\ 0\ \bar{1})$ which displays elongated eight-membered rings (widest dimensions ~19 Å × 4 Å) and has the total point symbol $\{4.8^2\}$.

The DMF molecules are protruding on both sides of the sheets (while remaining parallel to the sheet plane), the latter being tightly packed (KPI 0.65).

The last complex, $[H_2NMe_2]_2[(UO_2)_2(ADA)_3]\cdot 3H_2O$ (**5**), includes dimethylammonium cations formed in situ from DMF hydrolysis. The asymmetric unit contains two independent uranyl ions in similar environments, and three ADA^{2-} anions. In contrast to the previous complexes, all carboxylate groups are chelating here, so that each ligand bridges only two cations (Fig. 5). The U–O(carboxylate) bond lengths are in the range 2.436(3)–2.498(4) Å [average 2.472(19) Å]. A 2D network, parallel to $(1\ 0\ \bar{1})$, is formed in this case also but, instead of being one molecule thick as in **3** and **4**, the sheets in **5** are ~15 Å thick, with atom U2 and its symmetry equivalents located on the sheet sides with their equatorial planes close to the layer plane, and atom U1 and its equivalents located inside and perpendicular to the sheet plane. The total point symbol is $\{16\}\{8.16^2\}_2\{8\}_2$, with successive symbols for one of the ligands, the two metal centres, and the other two ligands. The dimethylammonium cations are hydrogen bonded to either two or three carboxylate oxygen atoms from the same sheet [N···O distances in the range 2.750(5)–3.066(6) Å], while inter-sheet hydrogen bonding interactions are mediated by the solvent water molecules [O···O distances in the range 2.738(8)–3.157(8) Å]. More specifically, the two hydrogen atoms bound to N1 form hydrogen bonds defining a second-order ring with the graph set descriptor $R_2^2(32)$, as can be seen in Fig. 5. The pattern built by the hydrogen atoms of N2 is different: one of them is involved in a bifurcated hydrogen bond with two oxygen atoms bound to the same uranium atom (only O16 is represented in Fig. 5) and it thus forms a $R_1^2(4)$ motif, while the two atoms together form a second-order ring with the descriptor $R_2^2(12)$. The solvent water molecules build a centrosymmetric hexamolecular cyclic pattern with descriptor $R_6^6(12)$, shown in Fig. 6. One hydrogen atom from each water molecule is involved in the building of the hexamer, and the second one is directed outward and linked to a carboxylate oxygen acceptor. The water molecules containing O17 and O19 are hydrogen bonded to two carboxylate oxygen atoms bound to the same uranium atom, thus giving an $R_3^3(8)$ ring, while that containing O18 is bound to one carboxylate oxygen atom coordinated to another metal centre. Chains of three hydrogen bonded water molecules are thus attached between carboxylate groups of the same layer, while the hydrogen bonds between the water molecules containing O18 and O19 link adjacent layers. No significant free space is present and the packing has a KPI of 0.66.

Nodal representations of the topologies observed in the present complexes, generated by the TOPOS software,[19] are shown in Fig. 7. The $[UO_2(ADA)]_2$ motif is present in structures **1**–**4**, but both the metal centre and the ligand are three-fold nodes in **1**, **2** and **4**, and four-fold ones in **3**. These dimers are linearly bound to one another in **1** and **2**, and the transformation of this ribbon arrangement into the 2D network in **4** involves the removal of the two internal bonds in one dimer out of two and their diversion toward adjacent ribbons, the lateral bonds being unchanged. The reason why this happens in **4** and not in **2**, notwithstanding the closeness of the DMF and NMP ligands, which are two *O*-donors of comparable bulk, is unclear; the additional 3d cations present during the synthesis of **4** may exert a structure-directing effect, although they are absent from the final compound. The network in **3** can be viewed as built from adjacent ribbons connected to one another by additional bonds resulting from the absence of terminal coordinating species. Here also, the presence of 4f cations during the synthesis may be invoked to explain the difference with **1**, these two compounds having been obtained in otherwise similar conditions, except that crystals of **1** were formed at 140°C and those of **3** on cooling the solution from this temperature. It is clear that even seemingly minor variations in the composition of the reaction mixtures can have marked effects on the dominant equilibria. With the metal centres being three-fold and the ligands two-fold nodes, the topology in **5** bears no clear relationship with the previous ones since the $[UO_2(ADA)]_2$ dimeric motif is no longer present. The network appears as a tessellation of 16- and 8-membered rings, the former winding and the latter close to planarity, and both slanted with respect to the sheet plane. This is the only case in this series of compounds in which the assembly is anionic, and the counter-ions, through both coulombic interactions and hydrogen bonding, are very likely to have a strong structure-directing effect.

The organic solvent used in the synthesis has clearly an effect either on the geometry of the polymeric assembly, or on the packing of these assemblies. An example of both is provided by complexes **1** and **2**: although the topology of the chains is identical in both cases, the coordinated solvent, water in **1** or NMP in **2**, occupies different locations within the polymers, and a second level of organization is provided by hydrogen bonding in **1**, resulting in the formation of hydrogen bonded sheets, while interactions between chains in **2** are only van der Waals or hydrophobic ones. With no molecule, either coordinated or free, involved in hydrogen bonding, the situation in the 2D compounds **3** and **4** is analogous to that in **2**, but complex **5** displays an intricate hydrogen bonding network involving both the dimethylammonium counter-ions and the lattice water molecules, the former having probably a structure-directing role and the latter uniting the 2D coordination polymers into a 3D framework. While the presence of coordinated or free water molecules is of course always possible due to the synthetic procedure used, water appears to be readily replaced as a ligand by coordinating solvents like NMP or DMF and, within this series, it is only present in one compound as a solvent. If the presence of hydrogen bonded molecules is an asset in the present cases, it must be noted that coordination of organic solvents is not necessarily always detrimental to an increase in dimensionality, as previously shown in the case of NMP in different uranyl–polycarboxylate systems.[8,11]

Luminescence Properties

Emission spectra under excitation at a wavelength of 420 nm in the solid state were recorded for all compounds except **3**, for which a sufficient amount of crystals could not be isolated, and they are represented in Fig. 8. Complexes **1**, **2** and **4**, in which the crystallographically unique uranium atom is in a pentagonal bipyramidal environment (with one chelating carboxylate) display very similar emission spectra, with the typical vibronic progression corresponding to the $S_{11} \rightarrow S_{00}$ and $S_{10} \rightarrow S_{0\nu}$ ($\nu = 0$–4) electronic transitions.[26] The maxima are at wavelengths of 489, 510, 533 and 558 nm for the four major peaks, with less well resolved bands at ~475 (in **1** and **2**), ~584–586 and ~613 nm. The number of donor atoms in the uranyl equatorial plane is known to affect these values,[27] and this is observed here since the emission spectrum of compound **5**, with two independent uranium atoms, both in hexagonal bipyramidal environment, is very different from those of the others. The wavelengths of the maxima are 463, 482, 502, 524 and 548 nm, and similar values have previously been found to be associated with octa-coordinate geometry in other polycarboxylate complexes (all measures having been made in the solid state and under the same conditions).[8,9,11,22] A similar displacement of the maxima positions towards slightly higher energy when going from five- to six-coordinate equatorial uranyl environments has also been observed in the 1,3-adamantanedicarboxylate series.[9] However, this trend is not general since a seven-coordinate uranium centre also bound to polycarboxylate anions was found to give values different from those in **1**, **2** and **4**,[28] and it appears also not to hold true in complexes with different ligands,[27] the maxima positions being sensitive to the strength of the equatorial donors.[27c] It may also be noted that the solid state emission spectra of uranyl ion complexes of *trans*-3-(3-pyridyl)acrylate, which contain uranium atoms in exclusively seven-coordinate environments, show rather poor resolution of the vibronic structure, presumably reflecting the superposition of slightly different emissions from the multiple, inequivalent uranyl units in the lattices, and the maxima positions seem to be intermediate between the two sets observed here.[29]

Conclusions

The present work is an extension of our previous investigation of cyclohexyl-based polycarboxylates as ligands for uranyl ions. The five complexes of ADA^{2-} which could be obtained are the first to be reported with uranyl ions, the only case with an actinide cation reported in the Cambridge Structural Database (CSD, Version 5.35)[30] being a 3D framework architecture involving thorium(IV),[31] a cation with a high coordination number whose structural features are closer to those of lanthanide ions than to those of the geometrically constrained uranyl ion. Variation of the experimental conditions gave complexes with different 1D or 2D polymeric arrangements. In contrast to the closely related ADC^{2-} ligand which gives 3D frameworks,[9] ADA^{2-} does not give any such an architecture under similar conditions, nor under any of the other conditions which have been tested. Formation of uranyl dimers through double carboxylate bridges is found in compounds **1**–**4**, in which the two carboxylate groups of the ligand are chelating (chelating and bridging in **3**) and bridging bidentate, as is ADC^{2-} in several of the complexes reported. The neutral assemblies formed in these cases, either ribbon-shaped or sheets, are close to planarity, an usual feature in uranyl structural chemistry. In contrast, the doubly chelating mode of the ligand gives an anionic, inflated 2D architecture in complex **5**. The organic solvent obviously plays an important part in the outcome of the reaction, whether it is present in the final compound as a co-ligand (complexes **2** and **4**) or undergoes hydrolysis to generate ammonium counter-ions (**5**), and additional metal cations present during the synthesis may also have an influence upon the nature of the material deposited, even if they are absent from the final compound. Hydrogen bonds have a significant effect on both the geometry of the coordination polymers formed, as exemplified by the probable structure-directing role of dimethylammonium cations in complex **5** (although cation–anion electrostatic interactions are probably the main force at play here), and the incorporation of the coordination polymers into larger architectures, 2D in **1** and 3D in **5**. Although such modifications of the synthetic conditions are useful to generate different complexes for one particular metal/ligand system, prediction of the specific geometry adopted in each case is of course elusive, particularly for such a flexible ligand. This was recently nicely illustrated in the very different system of 3d block metal cation complexes with mellitic acid.[32] The emission spectra of the complexes in the present series evidence the effect of the number of equatorial donors on the maxima positions.

References

1. For an overview of uranyl–organic frameworks, see: (*a*) C. L. Cahill, D. T. de Lill and M. Frisch, *CrystEngComm*, 2007, **9**, 15; (*b*) C. L. Cahill and L. A. Borkowski, in *Structural Chemistry of Inorganic Actinide Compounds*; S. V. Krivovichev, P. C. Burns and I. G. Tananaev, Eds.; Elsevier, Amsterdam, Oxford, 2007, ch. 11; (*c*) K. X. Wang and J. S. Chen, *Acc. Chem. Res.*, 2011, **44**, 531; (*d*) M. B. Andrews and C. L. Cahill, *Chem. Rev.*, 2013, **113**, 1121; (*e*) T. Loiseau, I. Mihalcea, N. Henry and C. Volkringer, *Coord. Chem. Rev.*, 2014, **266–267**, 69; (*f*) J. Su and J. S. Chen, *Struct. Bond.*, 2015, **163**, 265.
2. P. Thuéry, *CrystEngComm*, 2009, **11**, 232.
3. P. Thuéry, *Cryst. Growth Des.*, 2010, **10**, 2061.

4. P. Thuéry and B. Masci, *CrystEngComm*, 2012, **14**, 131.
5. P. Thuéry, M. Nierlich, B. W. Baldwin, N. Komatsuzaki and T. Hirose, *J. Chem. Soc., Dalton Trans.*, 1999, 1047.
6. P. Thuéry, *Cryst. Growth Des.*, 2014, **14**, 901.
7. P. Thuéry, *Cryst. Growth Des.*, 2014, **14**, 2665.
8. P. Thuéry and J. Harrowfield, *Cryst. Growth Des.*, 2014, **14**, 4214.
9. P. Thuéry, E. Rivière and J. Harrowfield, *Inorg. Chem.*, 2015, **54**, 2838.
10. For some recent examples, see: (*a*) Z. L. Liao, G. D. Li, X. Wei, Y. Yu and J. S. Chen, *Eur. J. Inorg. Chem.*, 2010, 3780; (*b*) Y. Xia, K. X. Wang and J. S. Chen, *Inorg. Chem. Commun.*, 2010, **13**, 1542; (*c*) I. Mihalcea, N. Henry and T. Loiseau, *Cryst. Growth Des.*, 2011, **11**, 1940; (*d*) I. Mihalcea, N. Henry, N. Clavier, N. Dacheux and T. Loiseau, *Inorg. Chem.*, 2011, **50**, 6243; (*e*) I. Mihalcea, N. Henry, C. Volkringer and T. Loiseau, *Cryst. Growth Des.*, 2012, **12**, 526; (*f*) C. Volkringer, N. Henry, S. Grandjean and T. Loiseau, *J. Am. Chem. Soc.*, 2012, **134**, 1275; (*g*) I. Mihalcea, N. Henry, T. Bousquet, C. Volkringer and T. Loiseau, *Cryst. Growth Des.*, 2012, **12**, 4641; (*h*) I. Mihalcea, C. Volkringer, N. Henry and T. Loiseau, *Inorg. Chem.*, 2012, **51**, 9610; (*i*) J. Olchowka, C. Falaise, C. Volkringer, N. Henry and T. Loiseau, *Chem.–Eur. J.*, 2013, **19**, 2012; (*j*) J. Olchowka, C. Volkringer, N. Henry and T. Loiseau, *Eur. J. Inorg. Chem.*, 2013, 2109; (*k*) P. M. Cantos and C. L. Cahill, *Acta Crystallogr., Sect. E*, 2014, **70**, m142; (*l*) I. Mihalcea, N. Henry and T. Loiseau, *Eur. J. Inorg. Chem.*, 2014, 1322.
11. P. Thuéry and J. Harrowfield, *Cryst. Growth Des.*, 2014, **14**, 1314.
12. R. W. W. Hooft, *COLLECT*; Nonius BV: Delft, The Netherlands, 1998.
13. Z. Otwinowski and W. Minor, *Methods Enzymol.*, 1997, **276**, 307.
14. G. M. Sheldrick, *Acta Crystallogr., Section A*, 2008, **64**, 112.

15. G. M. Sheldrick, *Acta Crystallogr., Sect. A*, 2015, **71**, 3.
16. G. M. Sheldrick, *Acta Crystallogr., Sect. C*, 2015, **71**, 3.
17. L. J. Farrugia, *J. Appl. Crystallogr.*, 1997, **30***,* 565.
18. K. Momma and F. Izumi, *J. Appl. Crystallogr.*, 2008, **41**, 653.
19. (*a*) V. A. Blatov, A. P. Shevchenko and V. N. Serezhkin, *J. Appl. Crystallogr.*, 2000, **33**, 1193; (*b*) V. A. Blatov, M. O'Keeffe and D. M. Proserpio, *CrystEngComm*, 2010, **12**, 44.
20. See, for example: (*a*) D. A. Buckingham, J. M. Harrowfield and A. M. Sargeson, *J. Am. Chem. Soc.*, 1974, **96**, 1726; (*b*) C. Paulet, T. Loiseau and G. Férey, *J. Mater. Chem.*, 2000, **10**, 1225; (*c*) W. Chen, J. Y. Wang, C. Chen, Q. Yue, H. M. Yuan, J. S. Chen and S. N. Wang, *Inorg. Chem.*, 2003, **42**, 944; (*d*) S. V. Ganesan, P. Lightfoot and S. Natarajan, *Solid State Sci.*, 2004, **6**, 757; (*e*) J. M. Harrowfield, B. W. Skelton, A. H. White and F. R. Wilner, *Inorg. Chim. Acta*, 2004, **357**, 2358; (*f*) J. Zhao, J. Li, P. Ma, J. Wang and J. Niu, *Inorg. Chem. Commun.*, 2009, **12**, 450; (*g*) A. Bilyk, J. W. Dunlop, R. O. Fuller, A. K. Hall, J. M. Harrowfield, M. W. Hosseini, G. A. Koutsantonis, I. W. Murray, B. W. Skelton, R. L. Stamps and A. H. White, *Eur. J. Inorg. Chem.*, 2010, 2106; (*h*) P. Thuéry, *Cryst. Growth Des.*, 2011, **11**, 2606; (*i*) P. Thuéry, *Cryst. Growth Des.*, 2011, **11**, 3282; (*j*) P. Thuéry, *Cryst. Growth Des.*, 2012, **12**, 499.
21. K. E. Knope and L. Soderholm, *Chem. Rev.*, 2013, **113**, 944.
22. P. Thuéry and J. Harrowfield, *CrystEngComm*, 2014, **16**, 2996.
23. J. A. Rusanova, E. B. Rusanov and K. V. Domasevitch, *Acta Crystallogr., Sect. C*, 2010, **66**, m207.
24. (*a*) M. C. Etter, J. C. MacDonald and J. Bernstein, *Acta Crystallogr., Sect. B*, 1990, **46**, 256; (*b*) J. Bernstein, R. E. Davis, L. Shimoni and N. L. Chang, *Angew. Chem. Int. Ed.*, 1995, **34**, 1555.

25. A. L. Spek, *J. Appl. Crystallogr.*, 2003, **36**, 7.

26. A. Brachmann, G. Geipel, G. Bernhard and H. Nitsche, *Radiochim. Acta*, 2002, **90**, 147.

27. (*a*) H. D. Burrows and M. da G. Miguel, *Adv. Colloid Interf. Sci.*, 2001, **89-90**, 485; (*b*) S. J. Formosinho, H. D. Burrows, M. da G. Miguel, M. E. D. G. Azenha, I. M. Saraiva, A. C. D. N. Ribeiro, I. G. Khudyakov, R. G. Gasanov, M. Bolte and M. Sarakha, *Photochem. Photobiol. Sci.*, 2003, **2**, 569; (*c*) M. P. Redmond, S. M. Cornet, S. D. Woodall, D. Whittaker, D. Collison, M. Helliwell and L. S. Natrajan, *Dalton Trans.*, 2011, **40**, 3914.

28. P. Thuéry, B. Masci and J. Harrowfield, *Cryst. Growth Des*., 2013, **13**, 3216.

29. P. Thuéry and J. Harrowfield, *Eur. J. Inorg. Chem.*, 2014, 4772.

30. (*a*) F. H. Allen, *Acta Crystallogr., Sect. B*, 2002, **58**, 380; (*b*) I. J. Bruno, J. C. Cole, P. R. Edgington, M. Kessler, C. F. Macrae, P. McCabe, J. Pearson and R. Taylor, *Acta Crystallogr., Sect. B*, 2002, **58**, 389.

31. K. M. Ok and D. O'Hare, *Dalton Trans*., 2008, 5560.

32. W. Clegg and J. M. Holcroft, *Cryst. Growth Des.*, 2014, **14**, 6282.

Table 1 Crystal data and structure refinement details

	1	**2**	**3**	**4**	**5**
Chemical formula	$C_{14}H_{20}O_7U$	$C_{19}H_{27}NO_7U$	$C_{15}H_{19.5}N_{0.5}O_6U$	$C_{17}H_{25}NO_7U$	$C_{46}H_{76}N_2O_{19}U_2$
M/g mol^{-1}	538.33	619.44	540.84	593.41	1437.14
Crystal system	Triclinic	Monoclinic	Monoclinic	Monoclinic	Monoclinic
Space group	$P\bar{1}$	$P2_1/c$	$C2/c$	$P2_1/n$	$P2_1/n$
a/Å	6.3900(3)	11.9941(6)	22.0938(11)	8.4491(6)	16.5765(4)
b/Å	9.8657(6)	12.8275(7)	9.4870(3)	25.5329(14)	13.5501(4)
c/Å	12.5336(9)	13.8161(7)	17.2485(9)	9.3969(8)	24.0775(8)
α/°	92.036(3)	90	90	90	90
β/°	97.215(4)	106.114(3)	117.251(2)	94.063(5)	95.800(2)
γ/°	94.435(4)	90	90	90	90
V/Å^3	780.72(8)	2042.15(19)	3214.1(3)	2022.1(3)	5380.4(3)
Z	2	4	8	4	4
D_{calcd}/g cm^{-3}	2.290	2.015	2.235	1.949	1.774
μ(Mo Kα)/mm^{-1}	10.427	7.988	10.128	8.063	6.084
F(000)	504	1184	2024	1128	2808
Reflections collected	45680	73806	59880	55830	170373
Independent reflections	4756	6227	4910	3835	13882
Observed reflections [$I > 2\sigma(I)$]	4311	4581	4324	3104	9742
R_{int}	0.069	0.050	0.037	0.074	0.081
Parameters refined	199	308	227	237	626
R_1	0.027	0.028	0.024	0.077	0.038
wR_2	0.058	0.057	0.057	0.193	0.090
S	1.013	0.959	1.073	1.189	0.984
$\Delta\rho_{\text{min}}$/e Å^{-3}	−2.03	−1.31	−1.19	−3.40	−1.25
$\Delta\rho_{\text{max}}$/e Å^{-3}	1.16	0.64	0.99	2.94	1.71

Figure Captions

Fig. 1 Top: View of complex **1**. Displacement ellipsoids are drawn at the 50% probability level. Carbon-bound hydrogen atoms are omitted. Symmetry codes: i = x, y – 1, z; j = –x, 1 – y, 1 – z; k = x, y + 1, z. Middle: View of the 1D assembly. Bottom: View of the packing with chains viewed end-on. The uranium coordination polyhedra are shown and hydrogen atoms are omitted in the last two views.

Fig. 2 Top: View of complex **2**. Displacement ellipsoids are drawn at the 40% probability level. The two positions of the disordered NMP molecule are represented. Symmetry codes: i = 1 – x, 1 – y, 1 – z; j = x – 1, y, z; k = x + 1, y, z. Middle: View of the 1D assembly. Bottom: View of the packing with chains viewed end-on. Hydrogen atoms are omitted in all views. Only one position of the NMP molecule is shown in the last two views.

Fig. 3 Top: View of complex **3**. Displacement ellipsoids are drawn at the 40% probability level. Symmetry codes: i = –x, 1 – y, 1 – z; j = x – 1/2, y + 1/2, z; k = 1/2 – x, 3/2 – y, 1 – z; l = x + 1/2, y – 1/2, z. Middle: View of the 2D assembly. Bottom: View of the packing with layers viewed edge-on. The solvent molecule and hydrogen atoms are omitted in all views.

Fig. 4 Top: View of complex **4**. Displacement ellipsoids are drawn at the 30% probability level. Symmetry codes: i = x – 1/2, 1/2 – y, z – 1/2; j = 1/2 – x, y + 1/2, 1/2 – z; k = x + 1/2, 1/2 – y, z + 1/2; l = 1/2 – x, y – 1/2, 1/2 – z. Middle: View of the 2D assembly. Bottom: View of the packing with layers viewed edge-on. Hydrogen atoms are omitted in all views.

Fig. 5 Top: View of complex **5**. Displacement ellipsoids are drawn at the 30% probability level. Water solvent molecules and carbon-bound hydrogen atoms are omitted. Hydrogen bonds are shown as dashed lines. Symmetry codes: i = $x - 1/2$, $1/2 - y$, $z - 1/2$; j = $3/2 - x$, $y - 1/2$, $3/2 - z$; k = $3/2 - x$, $y + 1/2$, $3/2 - z$; l = $x + 1/2$, $1/2 - y$, $z + 1/2$. Middle and bottom: Two views of the 2D assembly, face- and edge-on, respectively. Water solvent molecules and hydrogen atoms are omitted in the last two views.

Fig. 6 View of the hydrogen bonding pattern built by the lattice water molecules in complex **5**. Displacement ellipsoids are drawn at the 20% probability level. Hydrogen bonds are shown as dashed lines. Symmetry codes: m = $1 - x$, $1 - y$, $1 - z$; n = $x + 1$, y, z; o = $2 - x$, $1 - y$, $1 - z$. The two couples of atoms U2/U1^{m} and U1^{n}/U2^{o} pertain to different layers.

Fig. 7 Nodal representation of the networks in complexes **1**–**5**. Yellow: uranium, red: oxygen, blue: centroid of the ADA^{2-} ligand, dark red: centroid of the terminal ligand (NMP or DMF).

Fig. 8 Solid state emission spectra of complexes **1**, **2**, **4** and **5**. Excitation wavelength 420 nm.

Figure 1

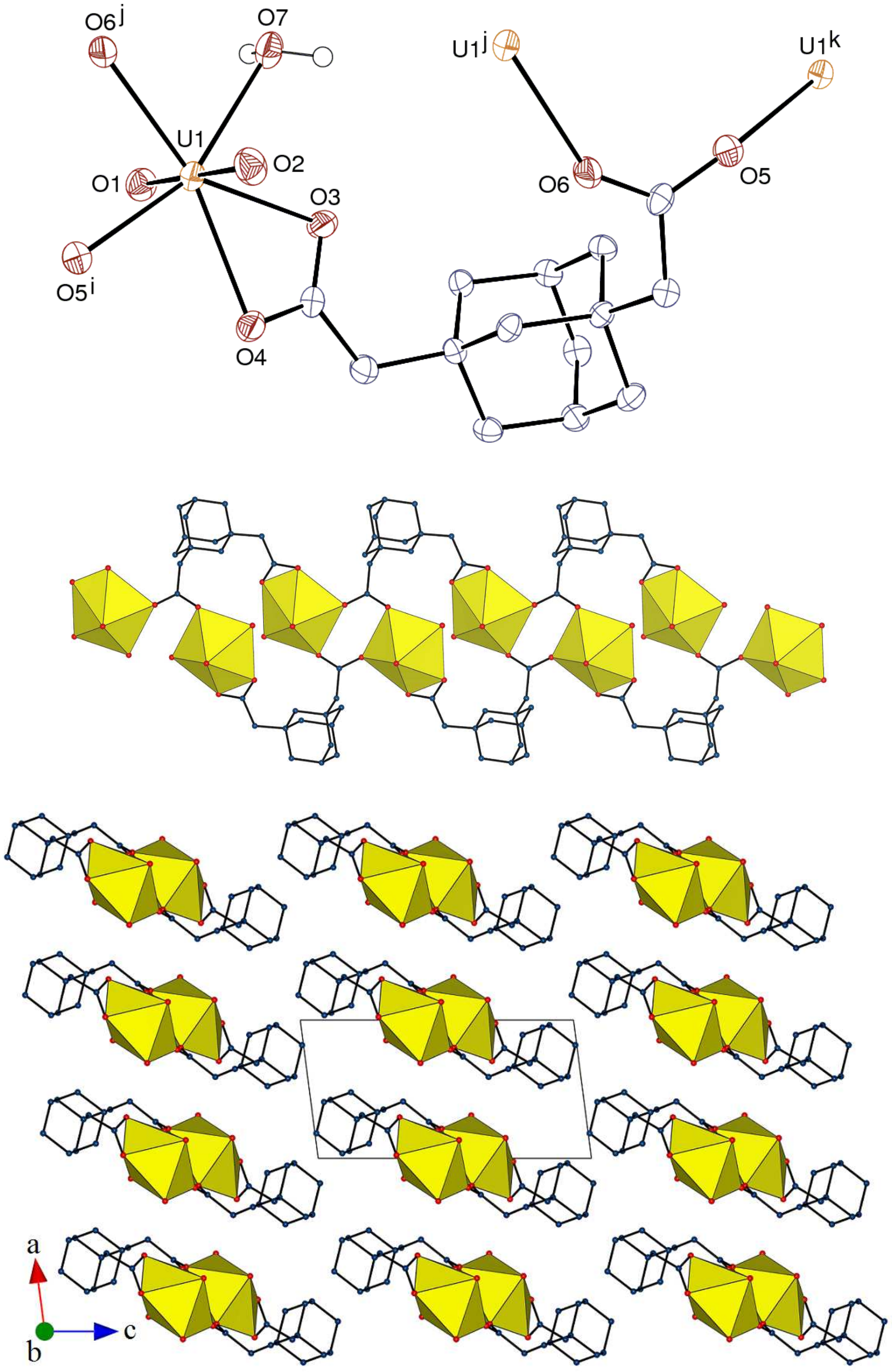

Figure 2

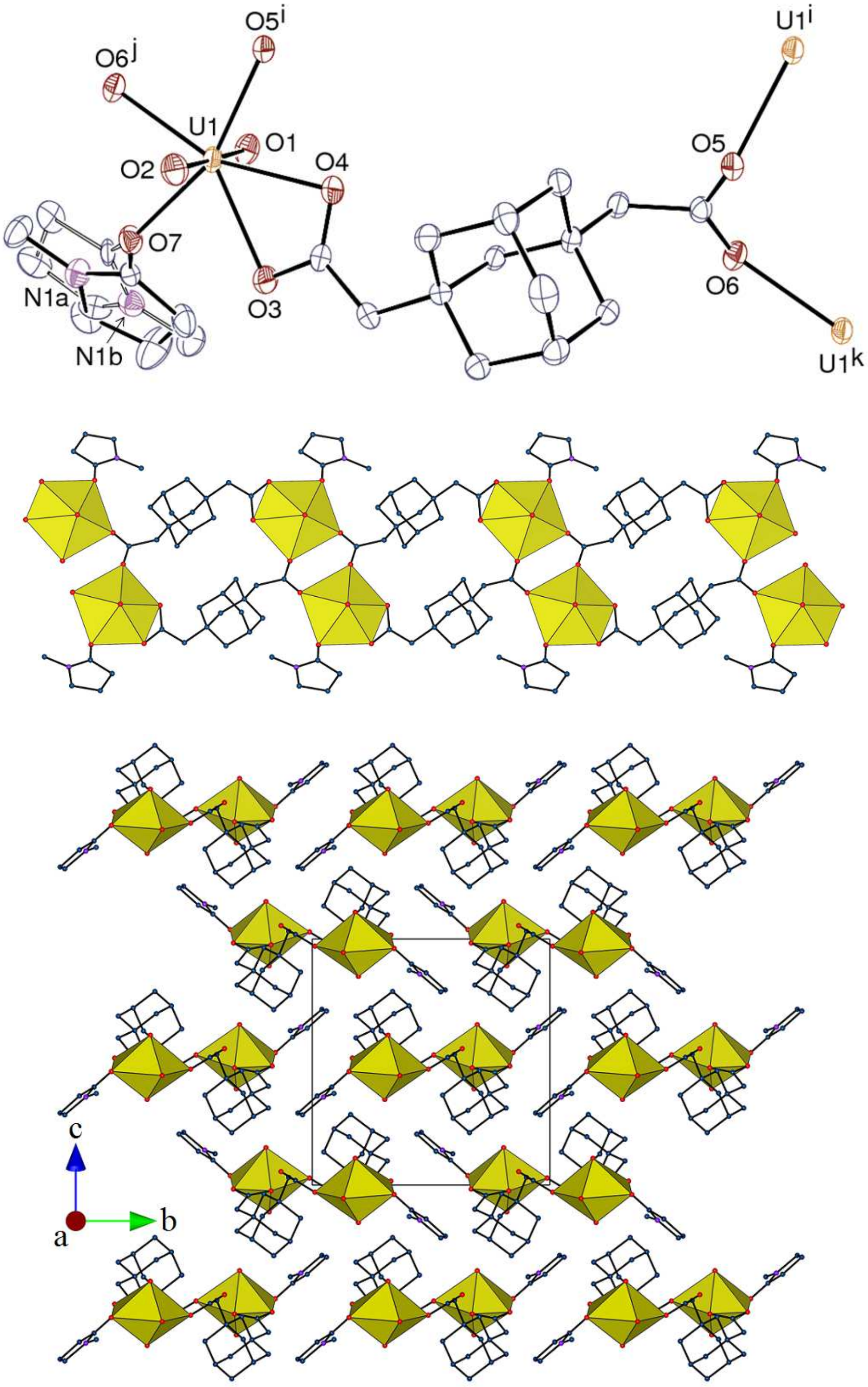
$\mathrm{O5}^{i}$
$\mathrm{O6}^{j}$
U1
O1
O2
O4
O7
O3
N1a
N1b
$\mathrm{U1}^{i}$
O5
O6
$\mathrm{U1}^{k}$
c
b
a

Figure 3

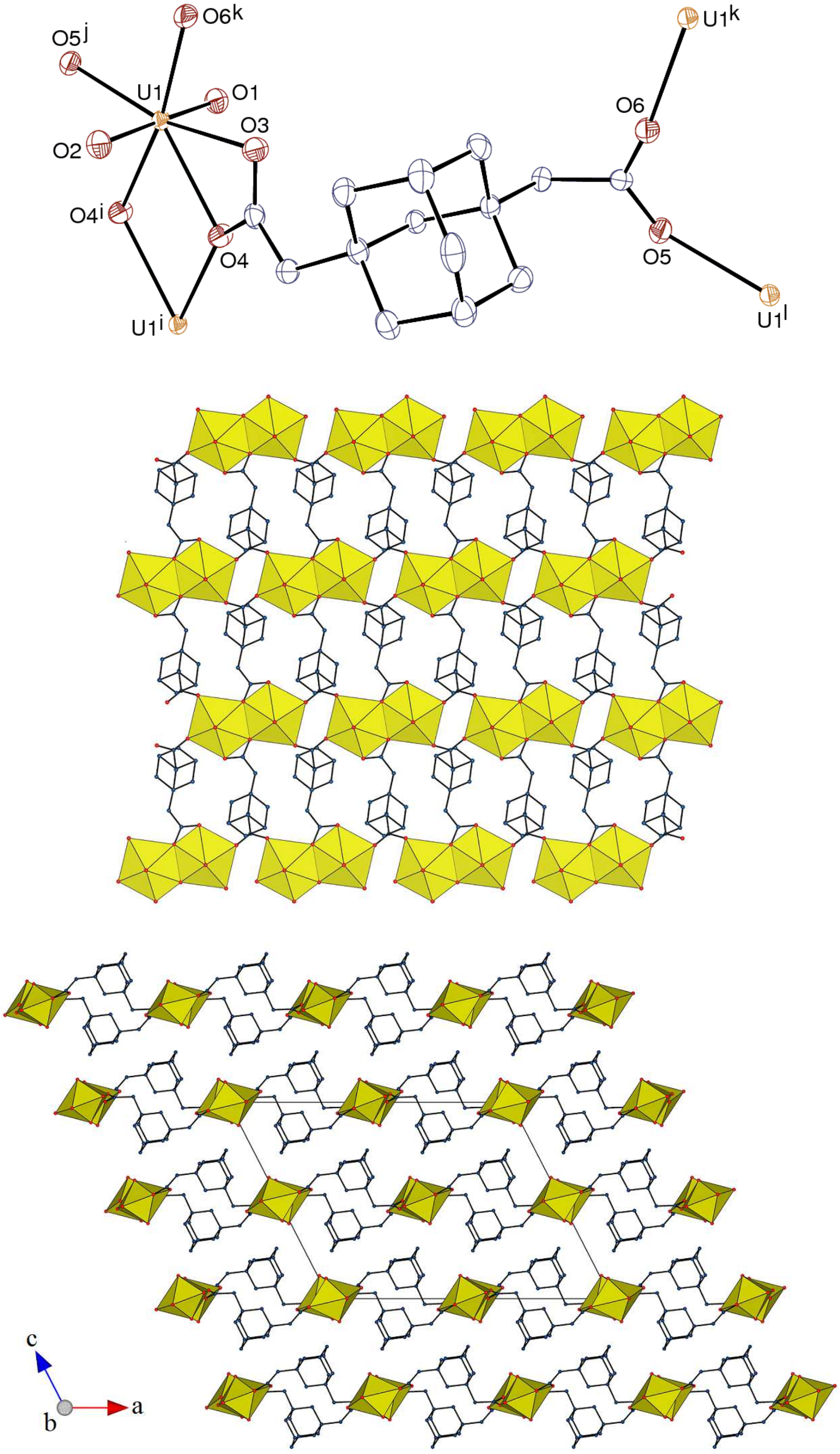
$\mathrm{O6}^{k}$
$\mathrm{O5}^{j}$
U1
O1
O3
O2
$\mathrm{O4}^{i}$
O4
$\mathrm{U1}^{i}$
$\mathrm{U1}^{k}$
O6
O5
$\mathrm{U1}^{l}$
c
b
a

Figure 4

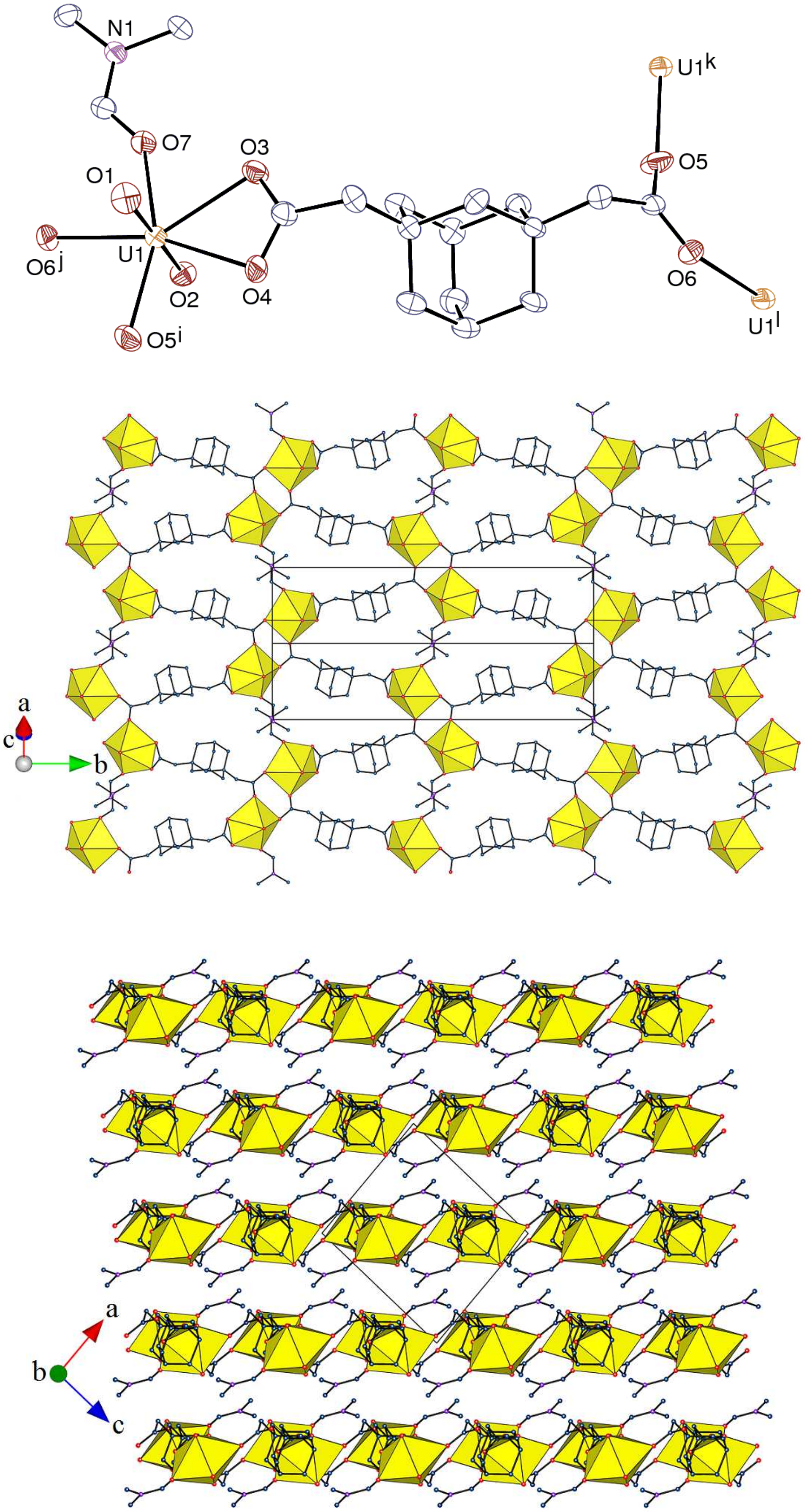

Figure 5

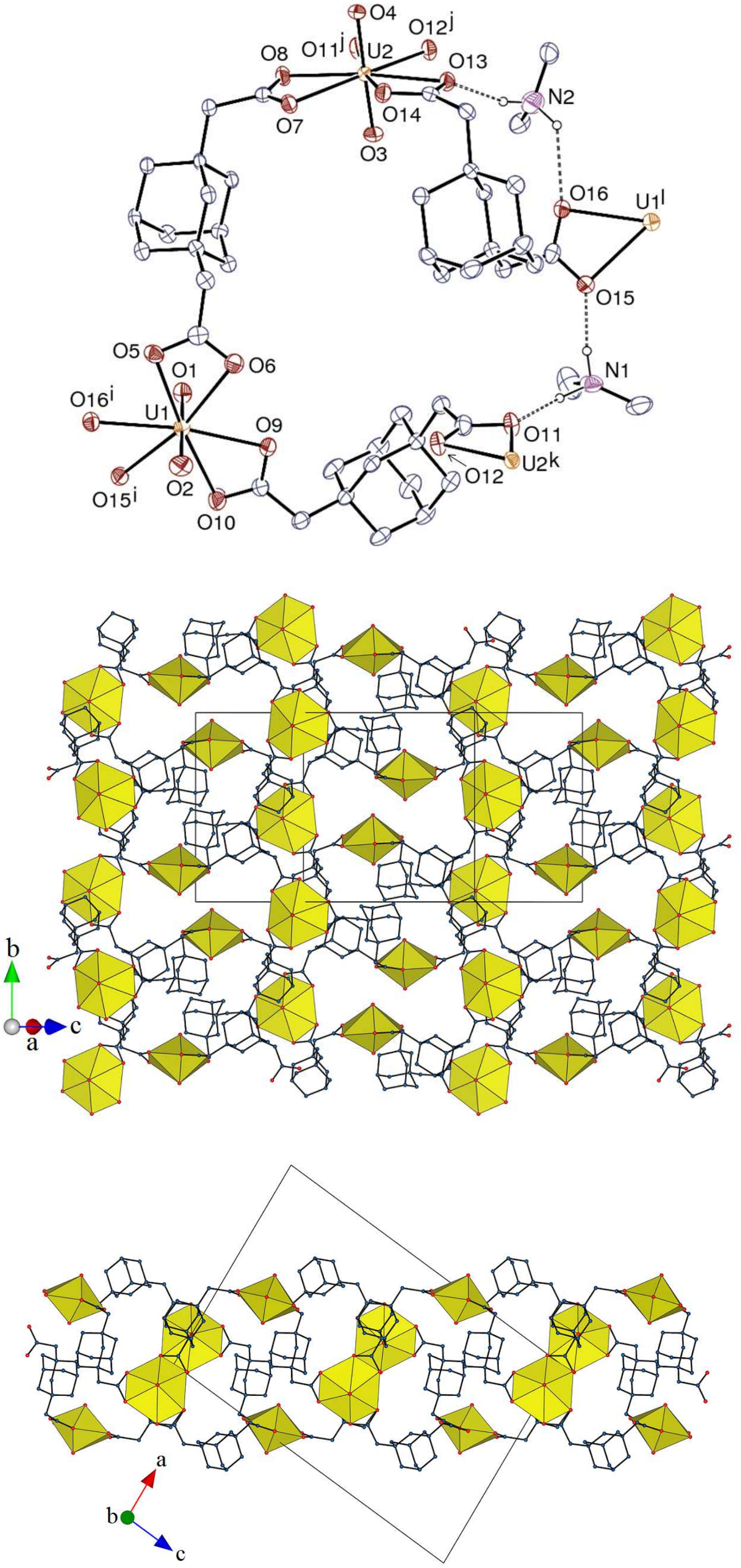
O4
O12^j
O11^j
U2
O8
O13
N2
O7
O14
O3
O16
U1^l
O15
O5
O1
O6
N1
O16^i
U1
O9
O11
O12
U2^k
O15^i
O2
O10
b
a
c
a
b
c

Figure 6

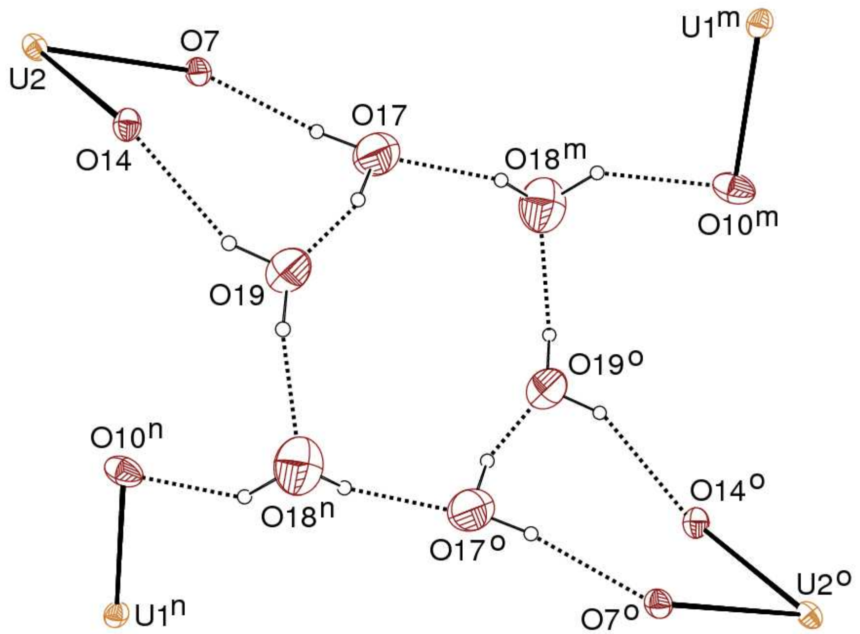
U2
O7
O14
O17
O18m
U1m
O10m
O19
O19o
O10n
O18n
O14o
O17o
U2o
O7o
U1n

Figure 7

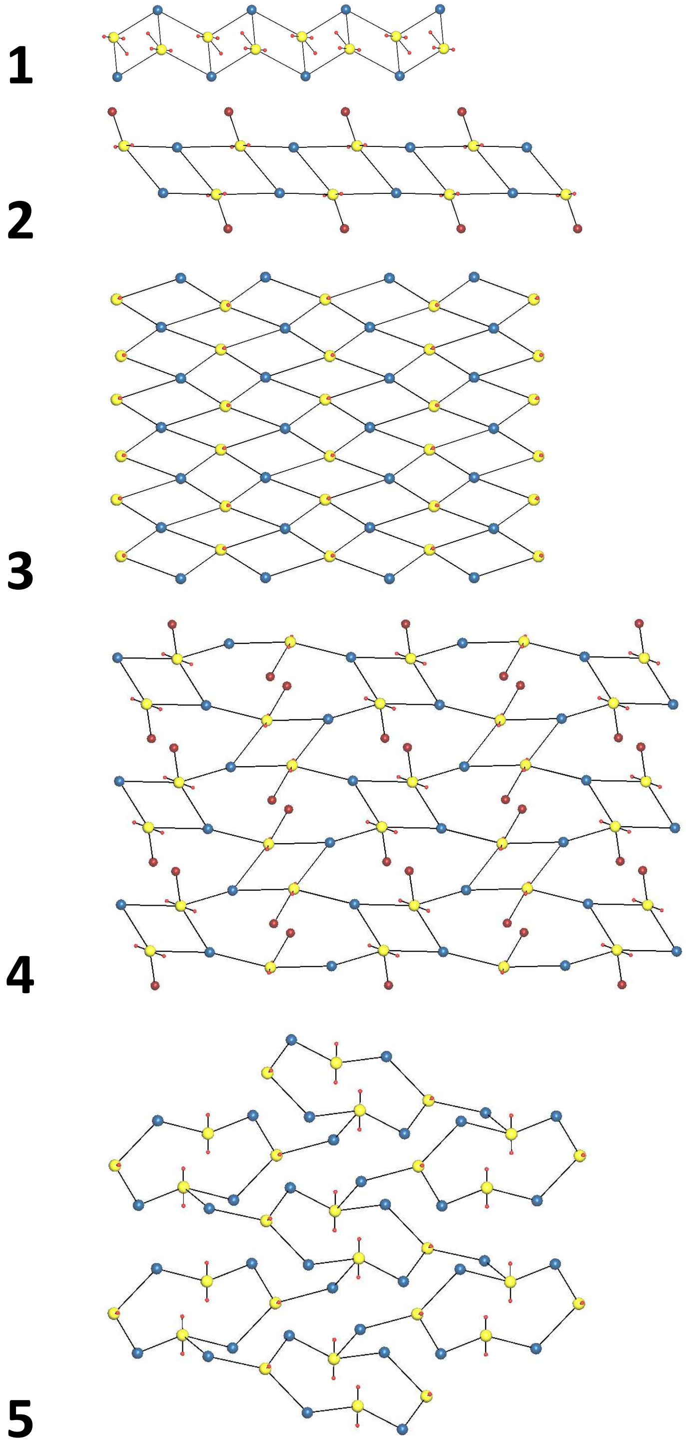

Figure 8

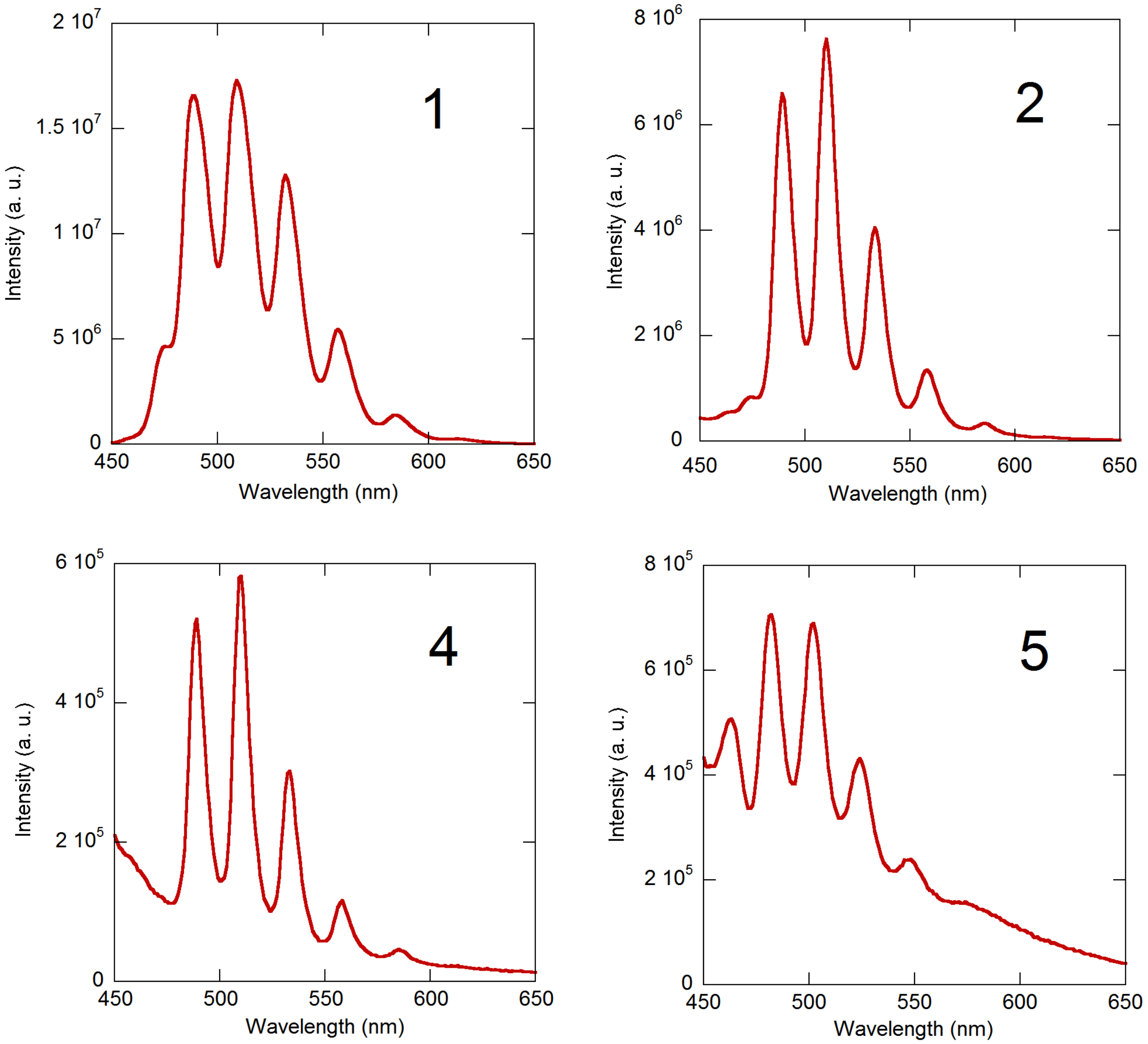
1
Intensity (a. u.)
0
5 10^6
1 10^7
1.5 10^7
2 10^7
450
500
550
600
650
Wavelength (nm)
2
Intensity (a. u.)
0
2 10^6
4 10^6
6 10^6
8 10^6
450
500
550
600
650
Wavelength (nm)
4
Intensity (a. u.)
0
2 10^5
4 10^5
6 10^5
450
500
550
600
650
Wavelength (nm)
5
Intensity (a. u.)
0
2 10^5
4 10^5
6 10^5
8 10^5
450
500
550
600
650
Wavelength (nm)

For Table of Contents Use Only

Solvent effects in solvo-hydrothermal synthesis of uranyl ion complexes with 1,3-adamantanediacetate

Pierre Thuéry and Jack Harrowfield

Uranyl ion complexes with 1,3-adamantanediacetate display different topologies arising from variations in coordination mode and the presence of additional ligands.